A Measure of Q-Convexity

Péter Balázs[1] and Sara Brunetti[2(✉)]

[1] Department of Image Processing and Computer Graphics, University of Szeged, Árpád tér 2, Szeged 6720, Hungary
pbalazs@inf.u-szeged.hu
[2] Dipartimento di Ingegneria dell'Informazione e Scienze Matematiche, Via Roma, 56, 53100 Siena, Italy
sara.brunetti@unisi.it

Abstract. We define new measures of convexity for binary images. The convexity considered here is the so called Q-convexity, that is, convexity by quadrants. This kind of convexity has been mostly studied in Discrete Tomography for its good properties, and permits to generalize h-convexity to any two or more directions. Moreover convex binary images are also Q-convex, and for these two classes similar properties hold. Here we present two measures based on the geometrical properties of "Q-convex shape" which have the following features: (1) their values range from 0 to 1; (2) their values equal 1 if and only if the binary image is Q-convex; (3) their efficient computation can be easily implemented.

1 Introduction

The measure of convexity is one of the most important shape descriptors used in digital image analysis [12]. Various continuous and discrete convexity measures have been proposed in image processing which can be grouped into different categories. Area based measures form one popular category [3,16,17], while boundary-based ones [18] are also frequently used. Other methods use simplification of the contour [13] or a probabilistic approach [14,15] to solve the problem. In discrete geometry, and especially in discrete tomographic reconstruction a straightforward alternative of the continuous convexity concept is the horizontal and vertical convexity (or shortly, h-convexity), arising inherently from the pixel-based representation of the digital image (see, e.g., [2,8,9]). A measure of horizontal (or vertical) convexity was introduced in [1], showing also that the aggregation of the measure in two dimensions can be a difficult task. In this paper we propose an immediate two-dimensional convexity measure, based on the concept of Q-convexity [5,6]. This kind of convexity has been mostly studied in Discrete Tomography for its good properties, and permits to generalize h-convexity to any two or more directions. Moreover convex binary images are also Q-convex, and for these two classes similar properties hold.

The notion of salient points of a Q-convex image has been introduced in [10,11] as the analogue of extremal points of a convex set. They have similar features, and in particular a Q-convex image is characterized by its salient points. Therefore, salient points have been employed for the random generation of

N. Normand et al. (Eds.): DGCI 2016, LNCS 9647, pp. 219–230, 2016.
DOI: 10.1007/978-3-319-32360-2_17

Q-convex images [7]. Further, as salient points can be generalized for any binary image, they have been studied to model the "complexity" of a binary image. In this paper, we focus on estimators of shape descriptors, in particular convexity estimators. The idea is to exploit the geometrical description of a binary image provided by salient and generalized salient points. The advantages of this approach are that normalization is straightforward; the measures are equal to 1 if and only if the binary image is Q-convex; the efficient computation of the measures can be easily implemented; and the measures are easy to generalize to any two or more directions.

2 Preliminaries

In this section we introduce the necessary notation and definitions. Any binary image F is a $m \times n$ binary matrix, and it can be represented by a set of cells/pixels (unit squares) or, equivalently, by a finite subset of $\mathbb{Z}^2$ contained in a lattice grid $\mathcal{G}$ (rectangle of size $m \times n$) up to a translation. Throughout the paper, we are going to use both representations as notation for the latter one is more suitable to describe geometrical properties whereas the images are illustrated as sets of cells. For our convenience, we use F for both the image and its representation.

Let us consider the horizontal and vertical directions, and denote the coordinate of any point M of the grid $\mathcal{G}$ by (x_M, y_M). Then, M and the directions determine the following four quadrants:

$$
\begin{aligned}
Z_0(M) &= \{N \in \mathcal{G} :\ 0 \le x_N \le x_M,\ 0 \le y_N \le y_M\} \\
Z_1(M) &= \{N \in \mathcal{G} :\ x_M \le x_N < m,\ 0 \le y_N \le y_M\} \\
Z_2(M) &= \{N \in \mathcal{G} :\ x_M \le x_N < m,\ y_M \le y_N < n\} \\
Z_3(M) &= \{N \in \mathcal{G} :\ 0 \le x_N \le x_M,\ y_M \le y_N < n\}.
\end{aligned}
$$

Definition 1. *A binary image F is Q-convex with respect to the horizontal and vertical directions if $Z_p(M) \cap F \neq \emptyset$ for all $p = 0, \ldots, 3$ implies $M \in F$.*

Figure 1 illustrates two Q-convex images.

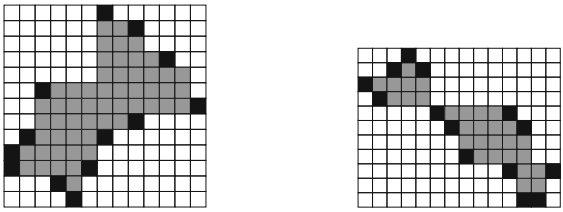

Fig. 1. Two Q-convex images. Salient points are indicated by black cells.

The Q-convex hull of F can be defined as follows:

Definition 2. *The Q-convex hull $\mathcal{Q}(F)$ of a binary image F is the set of points $M \in \mathcal{G}$ such that $Z_p(M) \cap F \neq \emptyset$ for all $p = 0, \ldots, 3$.*

Therefore, if F is Q-convex then $F = \mathcal{Q}(F)$. Differently, if F is not Q-convex, then $\mathcal{Q}(F) \backslash F \neq \emptyset$ (see Fig. 2). Denote the cardinality of F and $\mathcal{Q}(F)$ by α_F and $\alpha_{\mathcal{Q}(F)}$, respectively.

Definition 3. *For a given binary image F, its Q-convexity measure $\Theta(F)$ is defined to be $\Theta(F) = \frac{\alpha_F}{\alpha_{\mathcal{Q}(F)}}$.*

Since $\Theta(F)$ holds 1, if F is Q-convex, and $\alpha_{\mathcal{Q}(F)} \geq \alpha_F$, it ranges in $(0, 1]$. This Q-convexity measure corresponds to the classical convexity measure defined as the ratio between the area of the considered shape and the area of its convex hull. Similarly, $\Theta(F)$ is easy to compute but presents similar defects as does not detect defects in the shape which does not impact on the sizes α_F and $\alpha_{\mathcal{Q}(F)}$ (see Sect. 4 about the experiments with intrusions/protrusions images). Indeed, in the first case both α_F and $\alpha_{\mathcal{Q}(F)}$ differ by n so that Θ is close to 1, whereas in the second case α_F is close to $2/3\alpha_{\mathcal{Q}(F)}$ for n big.

Therefore, we are going to define a new measure based on the geometrical properties of the "shape".

Definition 4. *Let F be a binary image. A point $M \in F$ is a salient point of F if $M \notin Q(E \backslash \{M\})$.*

Denote the set of salient points of F by $\mathcal{S}(F)$ (or simply $\mathcal{S}$): of course $\mathcal{S}(\emptyset) = \emptyset$. In particular, it can be proven [10] that the salient points of F are the salient points of the Q-convex hull $\mathcal{Q}(F)$ of F. This means that if F is Q-convex, its salient points completely characterize F [6]. If it is not, there are other points belonging to the Q-convex hull of F but not in F that "track" the non-Q-convexity of F. These points are called generalized salient points. The generalized salient points $\mathcal{S}_g(F)$ of F are obtained iterating the definition of salient points on the sets obtained each time by discarding the points of the set from its Q-convex hull, i.e. using the set notation:

Definition 5. *If F is a binary image, then the set of its generalized salient points $\mathcal{S}_g(F)$ is defined by $\mathcal{S}_g(F) = \cup_k S(F_k)$, where $F_0 = F$, $F_{k+1} = \mathcal{Q}(F_k) \backslash F_k$.*

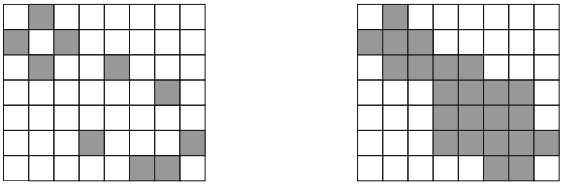

Fig. 2. Left: A non Q-convex binary image (all dark cells are salient points). Right: its Q-convex hull.

By definition, $\mathcal{S}(F) \subseteq S_g(F)$ and the equality holds when F is Q-convex. Moreover, as the points of $\mathcal{S}_g(F)$ are chosen among the points of subsets of $\mathcal{Q}(F)$, then $\mathcal{S}_g(F) \subseteq \mathcal{Q}(F)$.

We are now in the position to define two Q-convexity measures:

Definition 6. *For a given binary image F, its Q-convexity measure $\Psi_1(F)$ is defined by*

$$\Psi_1(F) = \alpha_{\mathcal{S}(F)}/\alpha_{\mathcal{S}_g(F)},$$

where $\mathcal{S}(F)$ and $\mathcal{S}_g(F)$ denote the sets of its salient and generalized salient points, respectively.

$\Psi_1(F)$ measures the Q-convexity of F in terms of proportion between salient points and generalized salient points. Indeed, if the generalized salient points are many with respect to salient points, then F is far to be Q-convex. This measure is purely qualitative because is independent from the size of the image.

Definition 7. *For a given binary image F, its Q-convexity measure $\Psi_2(F)$ is defined by*

$$\Psi_2(F) = \frac{\alpha_{\mathcal{Q}(F)} - \alpha_{\mathcal{S}_g(F)}}{\alpha_{\mathcal{Q}(F)} - \alpha_{\mathcal{S}(F)}},$$

where $\mathcal{Q}(F)$ denotes its Q-convex hull and $\mathcal{S}(F)$ and $\mathcal{S}_g(F)$ denote the sets of its salient and generalized salient points, respectively.

$\Psi_2(F)$ takes salient, and generalized salient points with respect to the Q-convex hull of the image into account. In other words, it measures the non-Q-convexity of F as the proportion of generalized salient points which are not salient and the points of the Q-convex hull which are not salient.

Since $\mathcal{S}(F) \subseteq \mathcal{S}_g(F) \subseteq \mathcal{Q}(F)$, both Q-convexity measures satisfy the following properties:

- the Q-convexity measure ranges from 0 to 1;
- the Q-convexity measure equals 1 if and only if F is Q-convex.

In particular, for $\Psi_1(F)$, since there are examples where $\mathcal{S}_g(F) = \mathcal{Q}(F)$ (for instance in the chessboard configuration), the ratio decreases with the inverse of the size of $\mathcal{Q}(F)$. For $\Psi_2(F)$, in the same case, we get exactly 0. We point out that we must have $\mathcal{S}(F) \subset \mathcal{Q}(F)$ in the definition of $\Psi_2(F)$, but $\mathcal{S}(F) = \mathcal{Q}(F)$ holds only for binary images of size smaller or equal to two. In these cases of course we also have $\mathcal{S}_g(F) = \mathcal{Q}(F)$, so that $\Psi_2(F)$ would be undefined.

3 Implementation

The measures Ψ_1 and Ψ_2 can be computed efficiently. Let us associate a boolean variable $V_p(M)$ to each point $M \in \mathcal{G}$, $p = 0, \ldots, 3$, such that $V_p(M) = 1$ if

$Z_p(M) \cap F \neq \emptyset$, else $V_p(M) = 0$. The variables can be easily computed by iteration:

$$V_0(x_M, y_M) = V_0(x_M - 1, y_M) \vee V_0(x_M, y_M - 1) \vee \text{“}(x_M, y_M) \in F\text{”}$$
$$V_1(x_M, y_M) = V_1(x_M + 1, y_M) \vee V_1(x_M, y_M - 1) \vee \text{“}(x_M, y_M) \in F\text{”}$$
$$V_2(x_M, y_M) = V_2(x_M + 1, y_M) \vee V_2(x_M, y_M + 1) \vee \text{“}(x_M, y_M) \in F\text{”}$$
$$V_3(x_M, y_M) = V_3(x_M - 1, y_M) \vee V_3(x_M, y_M + 1) \vee \text{“}(x_M, y_M) \in F\text{”}.$$

Finally the Q-convex hull of F is obtained by the formulas:

$$Q(F) = \{M \in \mathcal{G} : V_0(x_M, y_M) \wedge V_1(x_M, y_M) \wedge V_2(x_M, y_M) \wedge V_3(x_M, y_M)\},$$

and the computation requires a number of operations equal to the size of $\mathcal{G}$. The same variables permit to compute $\mathcal{S}(F)$ and, hence $\mathcal{S}_g(F)$, as follows. It can be proven [10] that M is a salient point of F if and only if there exists p such that $Z_p(M) \cap F = \{M\}$. So let $\mathcal{S}_p(F) = \{M \in F : Z_p(M) \cap F = \{M\}\}$; we get $\mathcal{S}(F) = \mathcal{S}_0(F) \cup \mathcal{S}_1(F) \cup \mathcal{S}_2(F) \cup \mathcal{S}_3(F)$. The set of salient points can be easily computed as we have:

$$\mathcal{S}_0(F) = \{M \in F : \neg V_0(x_M - 1, y_M) \wedge \neg V_0(x_M, y_M - 1)\}$$
$$\mathcal{S}_1(F) = \{M \in F : \neg V_1(x_M + 1, y_M) \wedge \neg V_1(x_M, y_M - 1)\}$$
$$\mathcal{S}_2(F) = \{M \in F : \neg V_2(x_M + 1, y_M) \wedge \neg V_2(x_M, y_M + 1)\}$$
$$\mathcal{S}_3(F) = \{M \in F : \neg V_3(x_M - 1, y_M) \wedge \neg V_3(x_M, y_M + 1)\},$$

where $\neg V_p$ is the negation of V_p. By definition, the set of generalized salient points is computed by iterating the computation of salient points on $\mathcal{Q}(F_k) \backslash F_k$ until the set reduces to the empty set. Therefore this computation depends on the size of $\mathcal{Q}(F)$ which bounds the number of iterations.

4 Case Study

We report on the behavior of the previous Q-convexity measures on the following representative configurations (F is a $n \times n$ binary image):

Chessboard. It is easy to check that if the items of F are arranged to form a chessboard, then $\mathcal{S}_g(F) = \mathcal{Q}(F)$. As a consequence, $\Psi_1(F) = \alpha_{\mathcal{S}(F)}/\alpha_{\mathcal{Q}(F)}$ depends on the size of $\mathcal{Q}(F)$ since $\alpha_{\mathcal{S}(F)} \in \{4, 6, 8\}$. This means that $\Psi_1(F)$ assigns different values to the same configuration decreasing for increasing sizes of F. In other words, bigger matrices are “less” Q-convex than smaller ones. Differently, $\Psi_2(F) = 0$ by definition. Therefore, the chessboard configuration is the “least” Q-convex configuration (for the Ψ_2 measure) (Fig. 3).

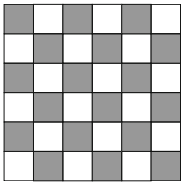

Fig. 3. $\Psi_1(F) = 0.176470$, $\Psi_2(F) = 0$.

Stripe Pattern. By counting reasoning, it is easy to see that if the items of F are arranged to constitute a stripe pattern, then $\alpha_{\mathcal{S}(F)} = 6$ whereas $\alpha_{\mathcal{S}_g(F)} = 6\lfloor\frac{n-1}{2}\rfloor + 4$, where $n \times n$ is the matrix size. Therefore $\Psi_1(F)$ decreases for n which increases. The behavior is similar to the chessboard case, but for the same size n, a chessboard configuration is "less" Q-convex than a stripe pattern configuration (in the first case the decrement is quadratic, in the second linear w.r.t n). For the Ψ_2 measure, the $\alpha_{\mathcal{Q}(F)}$ term dominates, so that its value is close to 1 for n big (for $n = 10$ $\Psi_2 = 0.58$, for $n = 50$ $\Psi_2 = 0.93$, for $n = 100$ $\Psi_2 = 0.965$). Hence, for this configuration the two measures give two different (opposite) "responses" (Fig. 4).

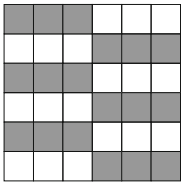

Fig. 4. $\Psi_1(F) = 0.375$, $\Psi_2(F) = 0.583333$.

Frame. If the items of F are arranged to form a frame, $\alpha_{\mathcal{S}(F)} = 4$ and $\alpha_{\mathcal{S}_g(F)} = 8$ or 5 if there is only one 0 item in F. Moreover, $\alpha_{\mathcal{Q}(F)} = n^2$. Therefore, $\Psi_1 = 1/2$ or $4/5$ in the latter case (constant), whereas Ψ_2 tends to 1 for increasing values of n. In both cases, the value is independent from α_F (from the "thickness" of the frame) (Fig. 5).

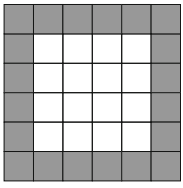

Fig. 5. $\Psi_1(F) = 0.5$, $\Psi_2(F) = 0.875$.

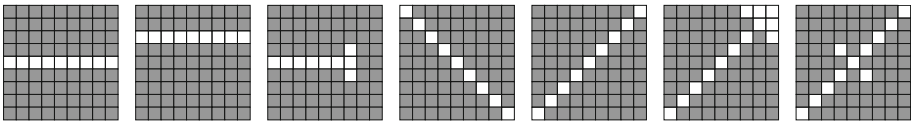

Fig. 6. Q-convexity values measured on intrusions images.

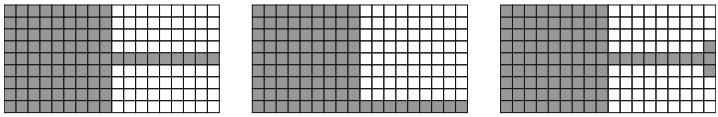

Fig. 7. Q-convexity values measured on protrusions images.

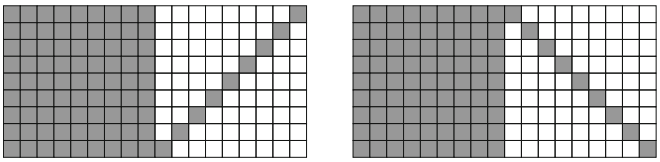

Fig. 8. Q-convexity values measured on protrusions images. $\Psi_1 = 0.550000$, $\Psi_2 = 0.921739$

"Bad" Configurations. The following figures illustrate examples of the application of the proposed Q-convexity measures for simple synthetic polygons: the values show the effects of rotation and translation of intrusions/protrusions images. In particular, consider the fourth image in Fig. 6. Note that $\alpha_{\mathcal{Q}(F)} = O(n^2)$; $\mathcal{S}(F)$ does not depend on the size of F; all (except the two on the first and last rows) the 0's item belong to $\mathcal{S}_g(F)$, and so $\alpha_{\mathcal{S}_g(F)} = O(n)$. We point out in addition that $\mathcal{S}_g$ does not depend on the "thickness" of the diagonal intrusion. Therefore, $\Psi_1(F)$ decreases when n increases; differently $\Psi_2(F)$ depends on $\mathcal{Q}(F)$ so that it is equal to 1 for $n = 2$ (and in fact F is Q-convex) and it is close to 1 for n big even if the diagonal intrusion is "thicker".

Consider the images illustrated in Fig. 8 (of course they have same measures by symmetry). Similar considerations hold with the difference that $\alpha_{\mathcal{S}(F)} = O(n)$ and the "thickness" of the protrusion affects $\alpha_{\mathcal{S}_g(F)}$ since it reduces items in $\mathcal{S}_g$. Therefore when n is big, Ψ_1 is greater or equal to $1/2$, and tends to 1 when the "protrusion" becomes very "thick", and Ψ_2 is close to 1.

In Fig. 10 we present the images used in [1] for the analysis of the horizontal and vertical convexity measure. For comparison, we also calculated the values of Q-convexity according to the measures Ψ_1 and Ψ_2. We deduce that the Q-convexity measures are in accordance with the horizontal and vertical convexity measures of [1] in the sense that higher Q-convexity values correspond to higher

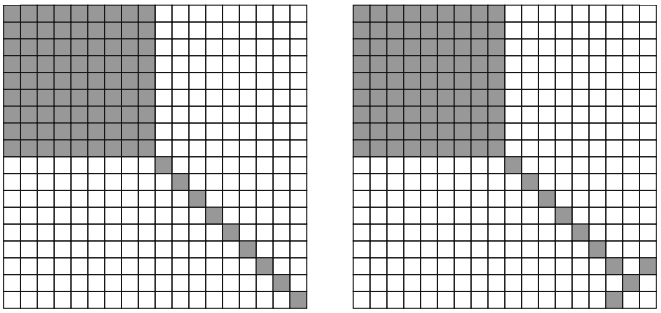

Fig. 9. Q-convexity values measured on protrusions images.

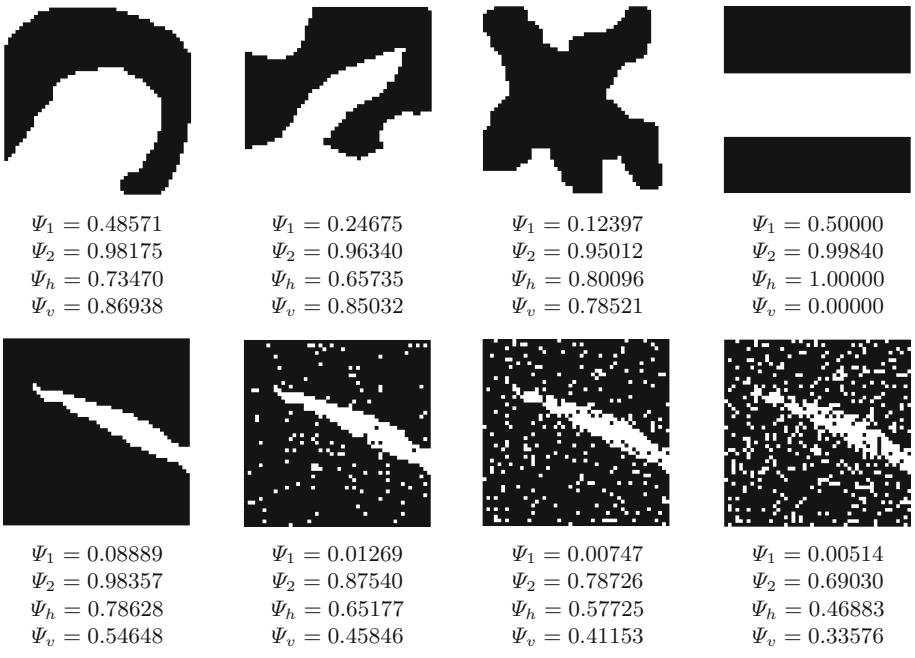

Fig. 10. Example binary images of size 50×50, with the Ψ_1 and Ψ_2 convexity values shown. Black pixels indicate object points. For comparison the horizontal (Ψ_h) and vertical (Ψ_v) convexity values are also given. Bottom row: same image without, and with 5 %, 10 %, and 20 % salt-and-pepper noise, from left to right, respectively.

h-convexity (v-convexity) values. Moreover, our measures visibly integrate the two one-directional measures (see especially the fourth image in the top row of Fig. 10). We also found that our measures scale well on noisy images (see bottom row of Fig. 10, for example). Finally let us notice that the values of the

Θ measure are $0.609828, 0.750000, 0.737407$ and 0.660000 for the binary images from left to right, respectively, in the top row, showing that the Θ measure does not "classify" the images in accordance with Ψ_1 and Ψ_2: for instance, according to Θ the first image is "less" Q-convex than the second one, whereas according to Ψ_1 and Ψ_2 the opposite holds.

5 Strongly Q-Convexity

The notion of Q-convexity can be extended to more than two directions [4,7]. Consider the horizontal, vertical and diagonal (i.e. $\boldsymbol{h} = (1,0)$, $\boldsymbol{v} = (0,1)$, $\boldsymbol{d} = (-1,1)$) directions. Let

$$\begin{aligned}
s_h^+(M) &= \{N \in \mathcal{G} \ : \ y_M = y_N \text{ and } \boldsymbol{h} \cdot \boldsymbol{ON} \geq \boldsymbol{h} \cdot \boldsymbol{OM}\} \\
s_h^-(M) &= \{N \in \mathcal{G} \ : \ y_M = y_N \text{ and } \boldsymbol{h} \cdot \boldsymbol{ON} \leq \boldsymbol{h} \cdot \boldsymbol{OM}\} \\
s_v^+(M) &= \{N \in \mathcal{G} \ : \ x_M = x_N \text{ and } \boldsymbol{v} \cdot \boldsymbol{ON} \geq \boldsymbol{v} \cdot \boldsymbol{OM}\} \\
s_v^-(M) &= \{N \in \mathcal{G} \ : \ x_M = x_N \text{ and } \boldsymbol{v} \cdot \boldsymbol{ON} \leq \boldsymbol{v} \cdot \boldsymbol{OM}\} \\
s_d^+(M) &= \{N \in \mathcal{G} \ : \ x_M + y_M = x_N + y_N \text{ and } \boldsymbol{d} \cdot \boldsymbol{ON} \geq \boldsymbol{d} \cdot \boldsymbol{OM}\} \\
s_d^-(M) &= \{N \in \mathcal{G} \ : \ x_M + y_M = x_N + y_N \text{ and } \boldsymbol{d} \cdot \boldsymbol{ON} \leq \boldsymbol{d} \cdot \boldsymbol{OM}\}
\end{aligned}$$

where O is the origin and $\cdot$ denotes the scalar product.

Definition 8. *An almost-semi-plane (or ASP) $\Pi(M)$ along the horizontal, vertical and diagonal directions is a zone $Z_p^{(i,j)}(M)$ ($i \neq j \in \{h,v,d\}$, $p \in \{0,\ldots,3\}$) such that for each direction k only one of the two semi-lines s_k^+ $s_k^-(M)$ is contained in $\Pi(M)$ for $k = h,v,d$.*

Let $\Pi_0(M)$ be the ASP containing $s_k^+(M)$ for each $k = h,v,d$. We denote the other almost-semi-planes encountered clockwise around M from $\Pi_1(M),\ldots,\Pi_5(M)$. In particular,

$$\begin{aligned}
\Pi_0(M) &= Z_2^{(dh)}(M) = \{N \in \mathcal{G} : \ x_M + y_M \leq x_N + y_N, y_M \leq y_N\} \\
\Pi_1(M) &= Z_2^{(vd)}(M) = \{N \in \mathcal{G} : \ x_M + y_M \leq x_N + y_N, x_M \leq x_N\} \\
\Pi_2(M) &= Z_1^{(h)}(M) = \{N \in \mathcal{G} : \ x_M \leq x_N, y_M \geq y_N\} \\
\Pi_3(M) &= Z_0^{(dh)}(M) = \{N \in \mathcal{G} : \ x_M + y_M \geq x_N + y_N, y_M \geq y_N\} \\
\Pi_4(M) &= Z_0^{(vd)}(M) = \{N \in \mathcal{G} : \ x_M + y_M \geq x_N + y_N, x_M \geq x_N\} \\
\Pi_5(M) &= Z_3^{(h)}(M) = \{N \in \mathcal{G} : \ x_M \geq x_N, y_M \leq y_N\}.
\end{aligned}$$

Definition 9. *A binary image F is strongly Q-convex around the horizontal, vertical and diagonal directions if $\Pi_p(M) \cap F \neq \emptyset$ for all $p = 0,\ldots,5$ implies $M \in F$.*

The definitions of Q-convex hull, salient and generalized salient points can be easily extended by replacing quadrants with ASP's. In order to compute them note that we can associate a boolean variable $V_p(M)$ to each point $M \in \mathcal{G}$ $p = 0, \ldots, 5$ such that $V_p(M) = 1$ if $\Pi_p(M) \cap F \neq \emptyset$, else $V_p(M) = 0$. Similar formulas to the two direction case can be derived to iteratively compute the variables. By their computation we can also derive the set of salient points $\mathcal{S}_p(M)$ $p = 0, \ldots, 5$ and finally the set of generalized salient points. Indeed, we can extend the proof in [10] to show that $M \in \mathcal{S}(F)$ iff there exists p such that $\Pi_p(M) \cap F = \{M\}$ and $\mathcal{S}(F) = \mathcal{S}(\mathcal{Q}(F))$.

We conducted the same experiments as in Sect. 4 for measuring the strongly Q-convexity of the images. We do not report all the results for space limits, but they are very similar with few differences.

For the intrusions test, as expected, the fourth image of Fig. 6 receives a better value, whereas the third and sixth are worse. For the protrusions test, values for images in Fig. 7 are worse because they are not strongly Q-convex, whereas values for images in Fig. 9 are exactly the same. The only significant difference concerns the second image in Fig. 8 for which $\Psi_1 = 0.571429$, $\Psi_2 = 0.975410$: indeed, $\mathcal{S} = 4$ and $\mathcal{S}_g = 7$ are constant (whereas they depend on n in case of Q-convexity w.r.t. horizontal and vertical directions), and, moreover, they score better values since the protrusion is in the diagonal direction.

Regarding the images of Fig. 10 we observed that the three directional Q-convexity values were more or less the same as in the two directional case, except the third image of the first row ($\Psi_1 = 0.08108$ and $\Psi_2 = 0.93621$ for the strongly Q-convexity measures) and the first image of the second row ($\Psi_1 = 0.11111$ and $\Psi_2 = 0.98717$). The reason is that the two images are "almost" convex in the diagonal direction.

6 Conclusion and Discussion

In this paper, we proposed two measures of convexity based on the notions of generalized salient points and Q-convex hull. First, we considered convexity in the horizontal and vertical directions and then we extended also the measures to a third diagonal direction. The experiments we conducted are promising as the measures correctly incorporate the convexity along the considered directions. In particular, measure Ψ_1 is more sensible to small modification of the shape, while Ψ_2 is more robust.

As a short discussion, let us notice here that a correcting factor could be used which takes into account also quantitative information. For example look at the images illustrated in Fig. 11, where Ψ_1 is constant $(1/2)$ and Ψ_2 is close to 1, since the geometry is preserved. But it would be desirable that the Q-convexity measures assign a bigger value to the configuration on the left of Fig. 11 and smaller to the configuration to the right. This can be obtained by multiplying the previous measures to the factor $\Theta(F) = \alpha_F / \alpha_{\mathcal{Q}(F)}$. For the image on the left $\alpha_{\mathcal{S}(F)} = 4$, $\alpha_{\mathcal{S}_g(F)} = 8$, $\alpha_{\mathcal{Q}(F)} = 64$, and $\alpha_F / \alpha_{\mathcal{Q}(F)} = 0.84345$, while for the image on the right $\alpha_{\mathcal{S}(F)} = 4$, $\alpha_{\mathcal{S}_g(F)} = 8$, $\alpha_{\mathcal{Q}(F)} = 64$, $\alpha_F / \alpha_{\mathcal{Q}(F)} = 0.34375$ which underpins

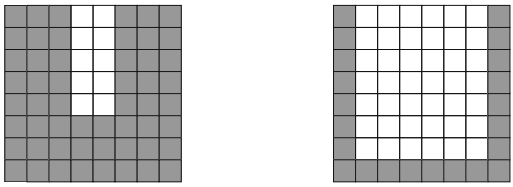

Fig. 11. Images to show the importance of the correcting factor. For the image on the left $\alpha_F/\alpha_{\mathcal{Q}(F)} = 0.84345$ while for the image on the right $\alpha_F/\alpha_{\mathcal{Q}(F)} = 0.34375$.

the above argument. Further work can be conducted to investigate the role of the correcting factor and to extend the measure to any two or more directions.

Acknowledgements. The collaboration of the authors was supported by the EXTREMA COST Action MP1207 "Enhanced X-ray Tomographic Reconstruction: Experiment, Modeling, and Algorithms". The research of Péter Balázs was supported by the OTKA K112998 grant of the National Scientific Research Fund.

References

1. Balázs, P., Ozsvár, Z., Tasi, T.S., Nyúl, L.G.: A measure of directional convexity inspired by binary tomography. Fundamenta Informaticae **141**(2–3), 151–167 (2015)
2. Barcucci, E., Del Lungo, A., Nivat, M., Pinzani, R.: Medians of polyominoes: a property for the reconstruction. Int. J. Imag. Syst. Technol. **9**, 69–77 (1998)
3. Boxter, L.: Computing deviations from convexity in polygons. Pattern Recognit. Lett. **14**, 163–167 (1993)
4. Brunetti, S., Daurat, A., Del Lungo, A.: An algorithm for reconstructing special lattice sets from their approximate X-rays. In: Borgefors, G., Nyström, I., Sanniti di Baja, G. (eds.) DGCI 2000. LNCS, vol. 1953, pp. 113–125. Springer, Heidelberg (2000)
5. Brunetti, S., Daurat, A.: An algorithm reconstructing convex lattice sets. Theor. Comput. Sci. **304**(1–3), 35–57 (2003)
6. Brunetti, S., Daurat, A.: Reconstruction of convex lattice sets from tomographic projections in quartic time. Theor. Comput. Sci. **406**(1–2), 55–62 (2008)
7. Brunetti, S., Daurat, A.: Random generation of Q-convex sets. Theor. Comput. Sci. **347**(1–2), 393–414 (2005)
8. Brunetti, S., Del Lungo, A., Del Ristoro, F., Kuba, A., Nivat, M.: Reconstruction of 4- and 8-connected convex discrete sets from row and column projections. Linear Algebra Appl. **339**, 37–57 (2001)
9. Chrobak, M., Dürr, C.: Reconstructing hv-convex polyominoes from orthogonal projections. Inform. Process. Lett. **69**(6), 283–289 (1999)
10. Daurat, A.: Salient points of Q-convex sets. Int. J. Pattern Recognit. Artif. Intell. **15**, 1023–1030 (2001)
11. Daurat, A., Nivat, M.: Salient and reentrant points of discrete sets. Electron. Notes Discrete Math. **12**, 208–219 (2003)

12. Gonzalez, R.C., Woods, R.E.: Digital Image Processing, 3rd edn. Prentice Hall, Harlow (2008)
13. Latecki, L.J., Lakamper, R.: Convexity rule for shape decomposition based on discrete contour evolution. Comput. Vis. Image Und. **73**(3), 441–454 (1999)
14. Rahtu, E., Salo, M., Heikkila, J.: A new convexity measure based on a probabilistic interpretation of images. IEEE Trans. Pattern Anal. **28**(9), 1501–1512 (2006)
15. Rosin, P.L., Zunic, J.: Probabilistic convexity measure. IET Image Process. **1**(2), 182–188 (2007)
16. Sonka, M., Hlavac, V., Boyle, R.: Image Processing, Analysis, and Machine Vision, 3rd edn. Thomson Learning, Toronto (2008)
17. Stern, H.: Polygonal entropy: a convexity measure. Pattern Recognit. Lett. **10**, 229–235 (1998)
18. Zunic, J., Rosin, P.L.: A new convexity measure for polygons. IEEE Trans. Pattern Anal. **26**(7), 923–934 (2004)